Depolarization of ferroelectric materials measured by their piezoelectric and elastic response

Z.W. He, O. Aktas, G. Linyu, L.-N. Liu, P.S. da Silva, F. Cordero, X.-M. Chen, X. Ding, E.K.H. Salje

PII: S0925-8388(22)02174-0

DOI: https://doi.org/10.1016/j.jallcom.2022.165783

Reference: JALCOM165783

To appear in: *Journal of Alloys and Compounds*

Received date: 31 March 2022
Revised date: 3 June 2022
Accepted date: 4 June 2022

Please cite this article as: Z.W. He, O. Aktas, G. Linyu, L.-N. Liu, P.S. da Silva, F. Cordero, X.-M. Chen, X. Ding and E.K.H. Salje, Depolarization of ferroelectric materials measured by their piezoelectric and elastic response, *Journal of Alloys and Compounds,* (2022) doi:https://doi.org/10.1016/j.jallcom.2022.165783

Depolarization of ferroelectric materials measured by their piezoelectric and elastic response

Z. W. He,[1] O. Aktas,[1,*] G. Linyu,[1] L.-N. Liu,[2] P. S. da Silva Jr.,[3] F. Cordero,[4] X.-M. Chen,[2] X. Ding,[1,*] and E. K.H. Salje[5]

[1]*State Key Laboratory for Mechanical Behavior of Materials, Xi'an Jiaotong University, Xi'an 710049, China*

[2]*School of Physics and information Technology, Shaanxi Normal University, Xi'an 710119, China*

[3]*Department of Physics, Federal University of São Carlos, 13565-905 São Carlos, São Paulo, Brazil*

[4]*Istituto di Struttura della Materia-CNR (ISM-CNR), Area della Ricerca di Roma-Tor Vergata, Via del Fosso del Cavaliere 100, I-00133 Roma, Italy*

[5]*Department of Earth Sciences, University of Cambridge, Cambridge CB2 3EQ, UK*

[*]oktayaktas@xjtu.edu.cn (O. Aktas), dingxd@mail.xjtu.edu.cn (X. Ding)

Depolarization in ferroelectric materials limits their piezoelectric applications and needs careful calibration for device constructions. With $BaTiO_3$ and $PbSc_{0.5}Ta_{0.5}O_3$ as prototypic ferroelectrics we demonstrate how to apply Resonant Piezoelectric Spectroscopy, RPS, to measure the direct and the converse piezoelectric effects as a function of temperature to detect depolarization via the collapse of the piezoelectric effect and the anomaly of elastic moduli. Comparison of the RPS data with in-situ d_{33} measurements on a $BaTiO_3$ ceramic shows that the temperature evolution of the longitudinal piezoelectric coefficient d_{33} can be determined with high accuracy. This makes RPS a complementary and convenient method for the investigation of polar phase transitions and the thermal evolution of the piezoelectric effect. Finally, the observation of an elastic anomaly concomitant to depolarization indicates that elastic measurements are an indirect means to measure the depolarization temperature in ferroelectrics.

1. Introduction

Applications of ferroelectrics as piezoelectric materials are vast as piezoelectricity can be exploited as sensors, transducers, energy harvesting, and so on. Along with current efforts to replace toxic lead-based materials, the increasing demand for piezo-devices has led to intensive research to find new materials that are environmentally friendly and suitable for future

applications [1-4]. These applications require knowledge about the thermal evolution of the piezoelectric coefficient (usually d_{33}) as well as the depolarization temperature(T_d), which often determines the upper temperature limit for their operation [1, 3, 5, 6, 7].

Perhaps the most comprehensive investigation of T_d by Anton *et al*. [7] found that measurements of thermally stimulated depolarization current and piezoelectric coefficients are the most accurate methods to determine T_d, which was defined as the temperature where the polarization shows the steepest decrease. Among these techniques, only the latter gives information about the evolution of piezoelectricity, which is crucial for high temperature applications. The piezoelectric coefficient can be measured by the Berlincourt method, or by indirect means including laser interferometers, impedance analyzer, and laser Doppler vibrometers [7, 8, 9, 10, 11]. The Berlincourt method is probably the most commonly used method. However, it is generally available only for room temperature measurements and *in-situ* thermal applications of this method are rarely reported in literature [12, 13, 14].

In this paper, we demonstrate resonant piezoelectric spectroscopy (RPS) a versatile and complementary technique to determine T_d and measure the thermal evolution of the piezoelectric coefficient d_{33}. Moreover, as RPS simultaneously provides piezoelectric and elastic properties, we were able to explore elastic measurements as a tool to detect depolarization and compare it with that obtained with the piezoelectric properties.

RPS was developed specifically to detect nano scale polar regions, such as twin walls, polar nano regions, and dipolar defects [15, 16, 17, 18, 19, 20]. Being an electrical analogue of Resonant Ultrasound Spectroscopy (RUS) [21, 22], RPS excites the elastic resonances of the sample through the piezoelectric effect (Fig. 1). Recently, it has been used for quantitative

evaluation of the piezoelectric effect (d_{33} coefficient) in a range covering 7 orders of magnitude with a sensitivity 2-3 orders of magnitude larger than conventional piezoelectric measurements [23]. Moreover, it was previously shown that RPS could detect depolarization in ferroelectric $PbSc_{0.5}Ta_{0.5}O_3$(PST) and $Na_{0.5}Bi_{0.5}TiO_3$ [24, 25]. However, in these measurements, samples were either poled just below their paraelectric-ferroelectric transition or by fields below their coercive field. More importantly, the common use of alumina waveguides [20, 26, 27] to transmit signal between the sample and detector for measurements above room temperature has hampered the analysis of the spectra. Here we used a direct contact configuration to overcome this drawback and obtain high quality elastic resonance spectra by using the converse or direct piezoelectric effects.

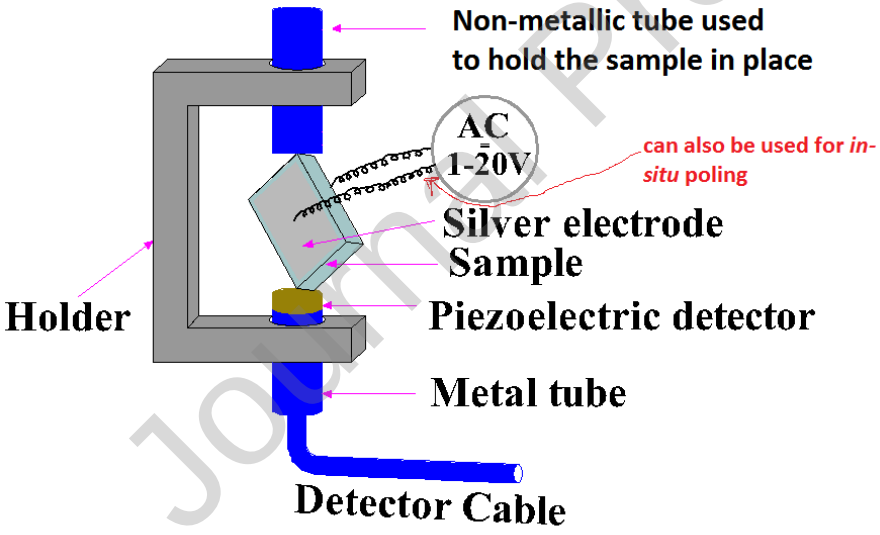

Fig. 1. Schematic of RPS used for investigation of direct and converse piezoelectric effects. An AC voltage applied across the sample through the wires attached to the electrodes on parallel faces of the sample generates mechanical resonances of the sample, which is picked up by the piezoelectric transducer, which acts as the detector. The same wires can be used for in-situ electrical poling of the sample. Alternatively, the AC voltage can be applied across the piezoelectric transducer to generate mechanical resonances. The voltage develops across the sample due to the direct piezoelectric effect of the sample and is collected via the wires attached to the electrodes on opposite faces of the sample. The same arrangement can be used for RUS measurements if a second transducer is attached to the upper tube in contact with the sample so that elastic resonances can be excited mechanically.

For this investigation, we chose two prototypic ferroelectric oxide ceramics with perovskite structure, namely $BaTiO_3$ and $PbSc_{0.5}Ta_{0.5}O_3$. The choice of these materials, among many types of ferroelectrics [28, 29, 30, 31, 32, 33, 34], stems from the fact that they are prominent compounds with well-known phase transitions. In fact, $BaTiO_3$ is the first ferroelectric oxide to be discovered [35, 36]. In $BaTiO_3$ the paraelectric-ferroelectric transition around 400 K corresponds to a structural change from cubic Pm-3m to tetragonal P4mm symmetry. They are also technologically important. In addition to its applications as a capacitor since 1950s [30], new solid solutions of $BaTiO_3$ are being synthesized for future applications, such as lead-free piezoelectrics, or those based on the electrocaloric, magnetoelectric, magnetic, and microwave dielectric properties [30, 32, 37, 38, 39, 40]. $PbSc_{0.5}Ta_{0.5}O_3$ has been used to clarify the origin of relaxor behavior in ferroelectrics as its B-site cation order Q_{od} (i.e., ordering of Sc and Ta ions) can be adjusted through thermal annealing or quenching [41, 42]. For samples with $Q_{od} > 55\%$, PST is ferroelectric (space group R3) with no obvious frequency dispersion with T_c = 295-300 K. It is a pyroelectric material [43] and has recently gained more importance as an electrocaloric material [44, 45].

In ceramics, the synthesis route and starting materials often affect the phase transition behavior and consequently dielectric, polar and piezoelectric properties [30, 46, 47, 48, 49, 50]. Therefore, we investigated samples of $BaTiO_3$ and $PbSc_{0.5}Ta_{0.5}O_3$ (with Q_{od} = 65%) whose phase transitions were previously investigated by other methods [51, 52]. For the $BaTiO_3$ ceramic, we additionally carried out in-situ direct piezoelectric effect measurements (by a Berlincourt-type d_{33} meter) for comparison with the piezoelectric properties obtained by RPS measurements (using both direct and converse piezoelectric effects). Results show that RPS can accurately measure the depolarization of poled ferroelectrics and determine the thermal evolution of d_{33},

while suggesting that the temperature dependence of the elastic modulus provides an indirect means to obtain a reasonable estimate for the depolarization temperature.

2. Methods

The $BaTiO_3$ ceramic was cut from a sample used in a previous investigation [51], where the synthesis of the sample by using a conventional solid-state reaction method was described. Sample dimensions were 6.45 x 4.39 x0.73 mm^3 and the density was 5.63 g/cm^3, corresponding to 93.6% of the theoretical value. The grain size of the sample was 42±15 μm. The oxygen vacancies were estimated to be less than 2500 ppm.

The $PbSc_{0.5}Ta_{0.5}O_3$ ceramic, synthesized by using the mixed-oxide method, is the same sample as used for Ref. [52] and is from the same batch of ceramics used in other investigations [24, 53, 43]. The dimensions of the sample were 6.51 x 6.61 x 0.69 mm^3 and the sample density was 8.72 g/cm^3, corresponding to 96.2% of the theoretical density. The grain size is 1-3 μm [43, 52]. The mixed-oxide method has been the traditional method for the synthesis of PST and generally leads to such small grain sizes [41, 43, 52]. Earlier investigation of the phase transition had no obvious sign of smearing of the transition related to the small grain size [52]. The chemical composition was checked by microprobe analysis, which indicated good uniformity of the Sc and Ta concentration and small (2%) variations for Pb, indicating PbO deficiency of up to ~2%, which can be inferred from the yellow coloration of the samples [41].

Prior to d_{33} and RPS measurements, the $BaTiO_3$ sample was poled in silicone oil with E = 20.5 kV/cm for 30 minutes at room temperature. The $PbSc_{0.5}Ta_{0.5}O_3$ sample was poled *in-situ* at 260 K with E = 13 kV/cm.

For $BaTiO_3$, a poled X-cut $LiNbO_3$ crystal with a diameter of 4 mm and thickness of 0.4 mm was used as piezoelectric detector (for converse piezoelectric effect) or generator (for direct piezoelectric effect). Measurements were carried out in an air-cooled furnace. A 15 minute settle time was allowed for thermal equilibration before collecting each RPS spectrum. For RPS measurements on PST, a PZT-5H ceramic with a diameter of 4 mm and a thickness of 0.4 mm was used as a detector. An illustration of the RPS holder, which consists of a piezoelectric transducer and sample in contact with the detector is shown in Fig. 1 (see caption for more details). For varying the temperature, measurements were carried out in a nitrogen gas-cooled furnace (Suns Electronic Systems EC1X). A 10 minute settle time was allowed for thermal equilibration before collecting the RPS spectra. All RPS measurements were computer controlled by using LabView.

The areas of RPS spectra of $BaTiO_3$ were calculated via numerical integration of the spectra with subtracted background. The IGOR PRO (Wavemetrics Inc.) code was used for data analysis. Resonance peak frequencies were determined by fitting an asymmetric Lorentzian function to individual resonance peaks. For the analysis of PST, Lorentzian fitting was additionally used to determine the inverse quality factor Q^{-1} (the full width at half maximum divided by resonance frequency) and the area of a resonance peak.

For in-situ measurements of the direct piezoelectric effect an experimental arrangement similar to the one described in Refs. [12, 13] was used. The sample was heated at a rate of 2 K/min and the d_{33} coefficient was measured in 2 K steps.

3. Results and Discussion

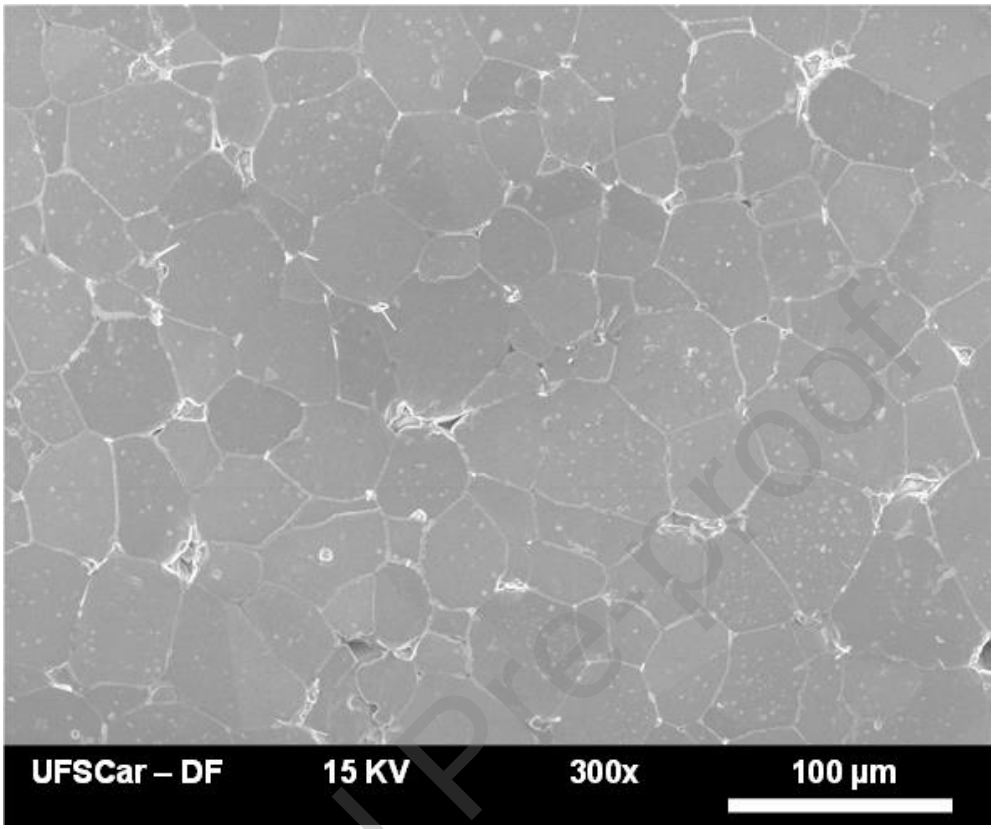

Fig. 2. SEM picture of BTO ceramic. Grains are coarse with an average size of 42±15 µm.

An SEM picture of the $BaTiO_3$ is displayed in Fig. 2. The sample has coarse grains with an average size of 42±15 µm. The dielectric constant of the sample was measured as 1750 at 1 kHz. In addition, the piezoelectric coefficient of the sample was 194.5 pC/N. These values are typical for a $BaTiO_3$ ceramic with coarse grains, which tend to have a dielectric constant ε = 1500-2500 and piezoelectric coefficient of ~190 pC/N [30, 48]. The grain size and oxygen vacancies are known to significantly affect the dielectric and piezoelectric properties of ceramics [30, 48, 54, 55, 56, 57, 58]. In the case of $BaTiO_3$, this was investigated in detail [48, 54, 55, 56], where dielectric constants of up to 8000 (in unpoled ceramics) and piezoelectric coefficients of 460 pC/N were reported with grain sizes of ~1 µm [55]. Similarly, large values of the dielectric

constant were observed in highly oxygen deficient samples [46, 51]. Such anomalous effects are negligible in the sample used in this work.

RPS spectra of poled $BaTiO_3$ ceramic were collected by using direct and converse piezoelectric effects, corresponding to panels (a) and (c) and panels (b) and (d) in Fig. 3, respectively. Spectra collected by both methods show the same resonances. The squared frequency of each resonance peak is proportional to an effective elastic modulus [21, 22]. All resonance frequencies show the same qualitative thermal behavior with temperature and reproduce earlier results obtained over a large frequency range by RUS, RPS, and other methods of elastic properties measurements [18, 51, 59, 60, 61]. These results illustrate the capability of RPS for the investigation of both direct and converse piezoelectric effects. Around 400 K, most resonances disappear on heating. This sharp drop of peak amplitudes is related to the depolarization of the sample occurring near the paraelectric-ferroelectric transition temperature. The resonances which are visible above T_c have different temperature dependence from those in the ferroelectric phase. Thus the ferroelectric-paraelectric transition at T_c 400 K is visible in both elastic and piezoelectric properties. Previous measurements of Young's modulus led to the same T_c [51].

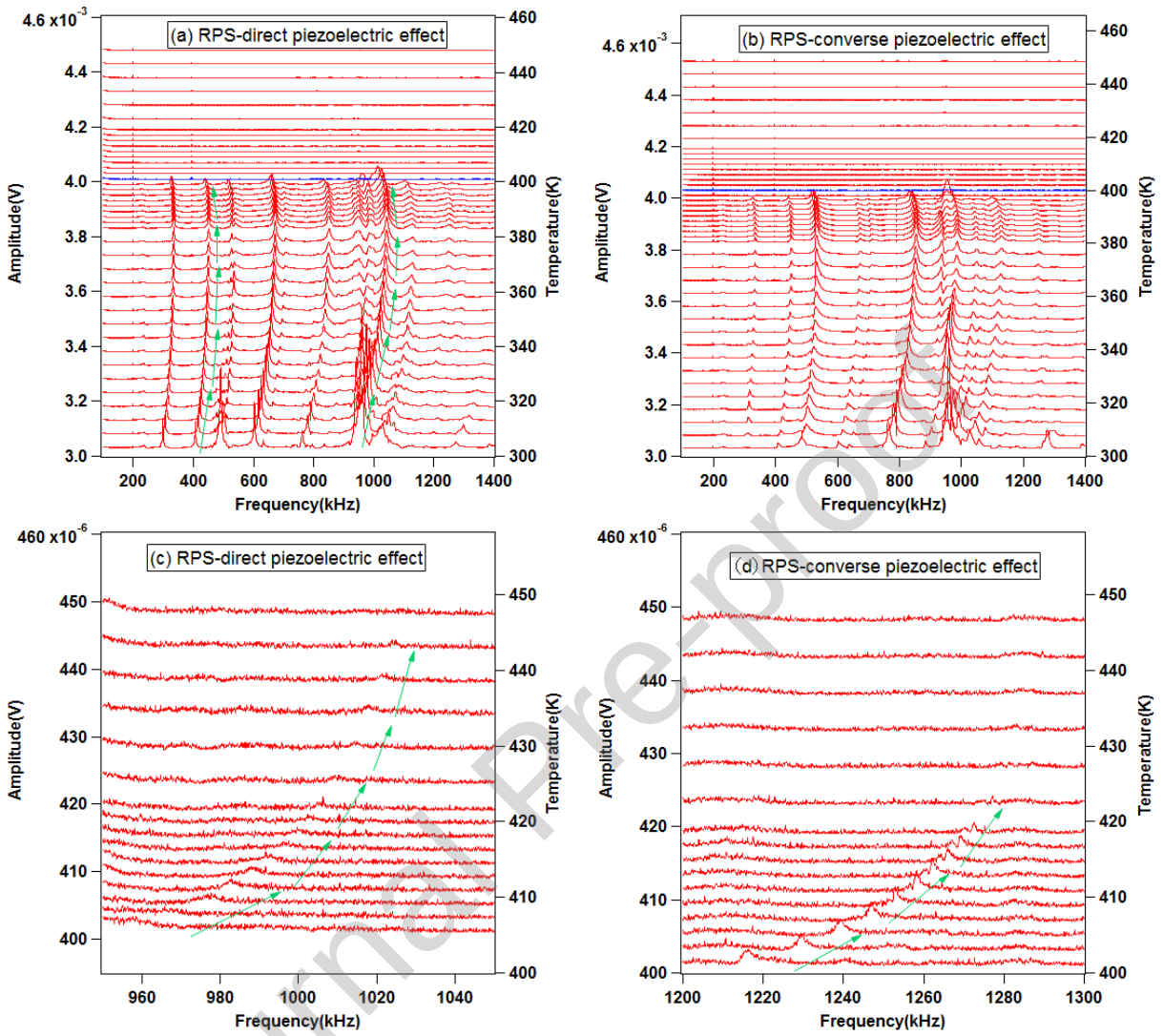

Fig. 3. RPS spectra of $BaTiO_3$ ceramic excited by (a), (b) direct and (c), (d) converse piezoelectric effects. Spectra were offset so that left axes represent amplitude and right axes represent temperature in all panels. Panels (c) and (d) show segments of spectra collected in the paraelectric phase (note the temperature axis on the right) and illustrate similar temperature evolution of two resonances. Spectra shown in blue in panels (a) and (b) were collected at the paraelectric-ferroelectric transition temperature T_c = 401 K. Green arrows are used as guides for the temperature evolution of elastic resonance peaks as examples.

To evaluate the RPS results quantitatively, we measured the temperature dependence of the piezoelectric coefficient d_{33} (see Fig. 4). As shown in Fig. 4(a), the depolarization occurs concomitant to a step change (and local minimum) in the squared frequency of an elastic resonance at T_c measured by RPS. This step change is similar to those reported in the literature

and results from the improper ferroelastic nature of the transition. Nonlinear softening in the paraelectric phase is related to precursors (nano scale regions with ferroelectric characteristics in the paraelectric phase) [18, 51, 59, 60, 61, 62]. These were visualized by Transmission Electron Microscopy [63, 64] and there is abundant literature reporting nanoscale polar regions not only with elastic but also piezoelectric [18, 65], second harmonic generation [66, 67], pyroelectric [68] and birefringence measurements [60]. Detailed discussion of the elastic behavior in improper ferroelectrics and improper ferroelastics can be found in [62].

A formal evaluation of the relationship between resonance peak areas and the effective piezoelectric coefficient has been performed recently, where the strain generated in RUS is used to calibrate the area of the RPS spectra [23]. In this methodology, the area of the RPS spectrum designates the average strain (via converse piezoelectric effect) or voltage (via direct piezoelectric effect) generated in an RPS measurement due to the effective piezoelectric coefficient of the sample, which depends on all piezoelectric coefficients. This averaging is used to minimize the effect of contact quality and geometry as well as piezoelectric anisotropy, which can significantly affect the peak amplitude of individual resonances every time the sample is remounted. In this work, RUS is not used for calibration. As the sample was not moved during the RPS measurements, which assures minimal influence of potential changes in the contact between the sample and the piezoelectric transducer, the temperature evolution of the spectrum area, i.e. generated strain or voltage, should be proportional to the temperature evolution of the effective piezoelectric coefficient. Note that another point to consider is the response function of the transducer, which is discussed in the following paragraphs.

The thermal evolution of the d_{33} coefficient (in Fig. 4(a)) is re-plotted in Fig. 4(b) after normalization with respect to the d_{33} value at 303 K. For comparison, the temperature dependence of the normalized RPS spectrum area (collected between 100 kHz and 1400 kHz) obtained by the direct piezoelectric effect (black triangles) is plotted together. Analysis of a lower frequency range (200-700 kHz) led to the same result (see Fig. A1). The dependencies are the same within 15%, indicating that RPS can quantitatively determine the temperature evolution of the d_{33} coefficient. The depolarization temperature, close to the ferroelectric-paraelectric transition temperature T_c, is also reproduced.

Although the effective piezoelectric coefficient obtained by the RPS measurement could contain contributions from the shear piezoelectric coefficients, the close agreement of in-situ d_{33} (as measured by the Berlincourt method) and d_{eff} extracted from RPS measurements indicate that the d_{33} coefficient makes the dominant contribution to d_{eff}. We attribute this to the fact that the $LiNbO_3$ disk (transducer) used as generator in the RPS measurements using the direct piezoelectric effect possesses its radial resonance [69, 70, 71] below 1 MHz while its thickness resonance [69, 70, 71] is above 5 MHz. Thus, the transducer generates a large stress in the direction of the electrodes that are on the large surfaces of the sample and is more sensitive to longitudinal vibrations in the frequency range investigated by the RPS measurements. Additionally, we consider the temperature dependence of the $LiNbO_3$ transducer used in our measurements as it is kept inside the furnace during heating of the sample. However, the effect of temperature on the piezoelectric coefficients of $LiNbO_3$ is negligible [72]. This indicates that RPS is capable of obtaining the quantitative values of d_{33} as a function of temperature with a suitable transducer, provided that the area of an RPS spectrum collected at a certain temperature (for example, room temperature) is scaled with respect to d_{33} measured at the same temperature

by using a quasi-static d_{33} meter. The scaling factor then can be used to scale the areas under the spectra collected as a function of temperature. Testing this approach on more samples is necessary to generalize this approach.

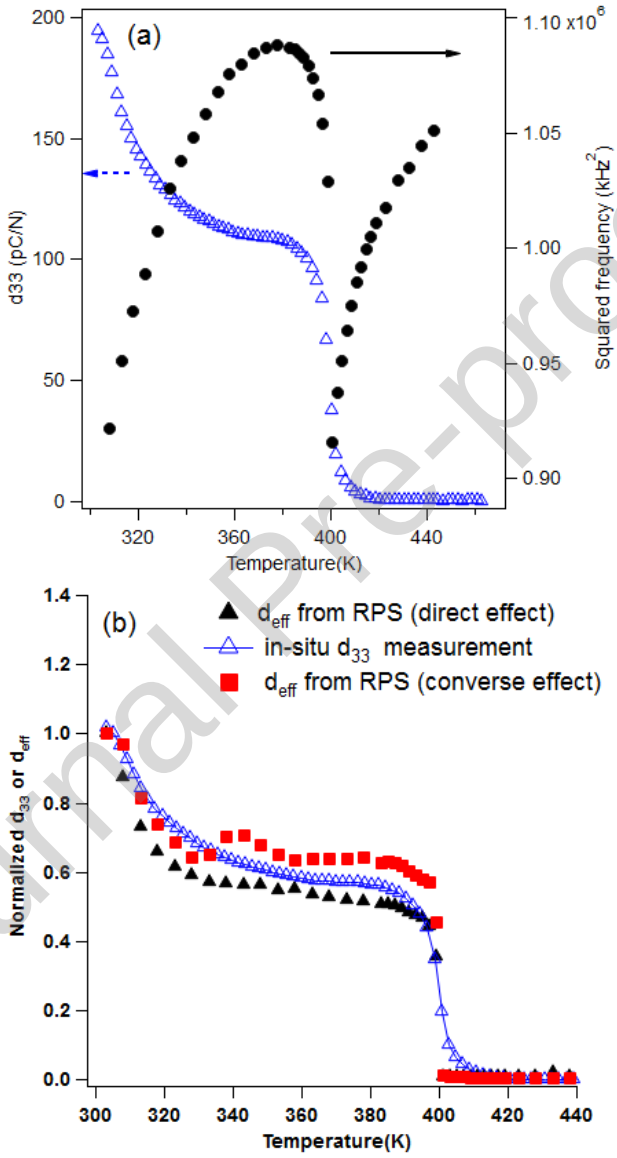

Fig. 4. Thermal evolution of piezoelectric and elastic properties in a $BaTiO_3$ ceramic. (a) Longitudinal piezoelectric coefficient (d_{33}) (blue triangles) measured by in-situ direct piezoelectric coefficient measurements and the squared frequency of an elastic resonance frequency (black circles). This resonance corresponds to the one in in Figs. 2(a) and (c) with its temperature evolution illustrated with green arrows and has a frequency of f>900 kHz in the temperature range investigated. (b) Comparison of normalized d_{33} coefficient (from in-situ Berlincourt-type measurements) with effective direct and converse piezoelectric coefficients obtained from RPS spectra.

The temperature evolution of the converse piezoelectric coefficient measured by RPS follows similar temperature dependence. The evaluation of a smaller segment of the spectra (200-700 kHz) led to a monotonous temperature dependence up to T_c. Note that, although direct and converse piezoelectric effects are thermodynamically identical and are equal in simple materials such as piezoelectric quartz [73], domain walls and other factors, such as boundary conditions and field amplitude, [73, 74, 75, 76] tend to lead to discrepancies [77]. Similar effects (i.e. boundary conditions, field amplitudes) may play a role in the vicinity of T_c, including a ~10 K range just above T_c, where d_{33} and d_{eff} show larger deviations. The geometry used in RPS (Fig. 1) and d_{33} measurements (in which stress is applied along the large surfaces of the sample) are entirely different. Precursors are ferroelectric and ferroelastic and they are expected to respond to stress [78], however it is currently unclear how they respond to stress under different experimental geometries and stress amplitudes. The observation of the piezoelectric effect in the paraelectric phase is consistent with the literature [18, 23, 66, 68].

We next examine the depolarization in $PbSc_{0.5}Ta_{0.5}O_3$ [41, 42, 44, 45] with B-site cation order Q_{od} = 0.65 [24, 52, 53, 43]. Extensive investigation of the phase transition behavior and dielectric and polar properties were previously carried out on the same sample [29] or those from the same batch of ceramics [24, 43]. The dielectric constant and polarization of these samples were consistent with that reported for samples with comparable PbO loss, cation order, and grain size [41]. Elastic, caloric, and polarization measurements on the same sample led to the transition temperature T_c = 295 K. Here, we compare the depolarization behavior as seen by RPS with these earlier results. As the paraelectric-ferroelectric transition temperature is just below room temperature, poling was done *in-situ* at 260 K with a DC field of E = 13 kV/cm. RUS was done

under *in-situ* electrical poling to investigate domain switching and domain wall pinning in a $BaTiO_3$ single crystal [79]. This means that RPS could be used to decipher the mechanical response of materials to electric fields, although not explored in this work (note that RPS is electrical analogue of RUS). The electric field was applied across the sample via the wires attached to the sample electrodes, which are also used to investigate the (converse) piezoelectric effect (Fig. 1). Fig. 5(a) depicts successful poling of the sample via the comparison of the peak amplitudes of resonances before (blue curve) and after poling (red curve), with the latter being 2-3 orders of magnitude higher than the former. One can see noticeable changes in the elastic resonance frequencies after poling, for example, just below 400 and 600 kHz, reflecting changes in the mechanical properties of the sample due to ferroelectric switching [79].

The transition is improper ferroelastic [24] and elastic softening mechanisms similar to those of $BaTiO_3$ apply. The depolarization of the sample near the transition leads to the collapse of elastic resonances (Fig. 5 (b)) and is accompanied by a sharp drop in the elastic modulus (Fig. 5(c)), similar to earlier results. In Fig. 5(d), the evolution of the RPS peak area of the resonance peak shown with green arrows in panel (a) corresponds to the depoling of the sample and is in perfect agreement of the depolarization seen by the thermal evolution of the remnant polarization of the same sample [29]. Thus, similar to the results on $BaTiO_3$, the depolarization is detected by both piezoelectric and elastic properties.

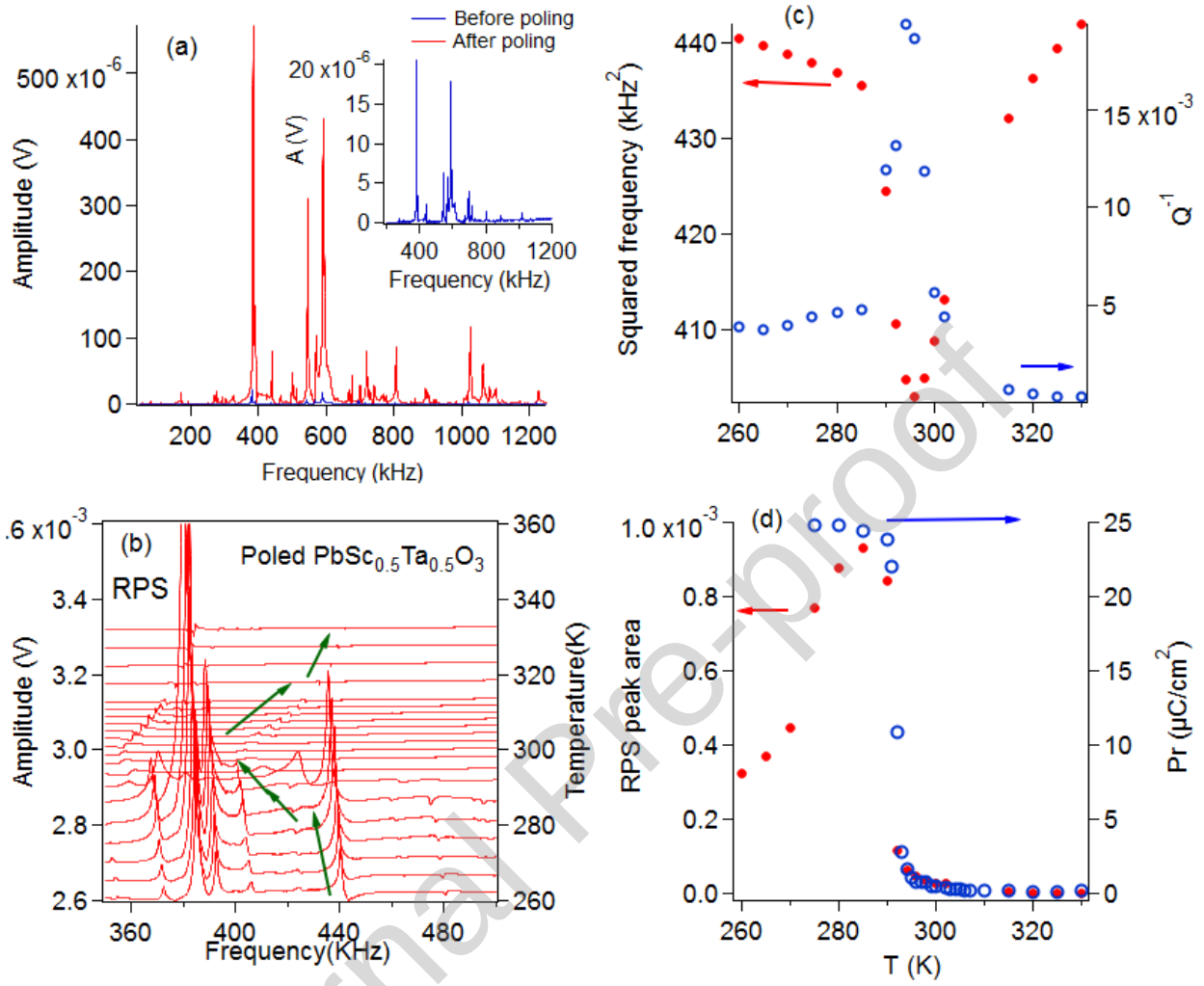

Fig. 5. Depolarization behavior of ferroelectric $PbSc_{0.5}Ta_{0.5}O_3$ at the paraelectric-ferroelectric transition T_c = 295 K. (a) In-situ electrical poling of PST with E = 13 kV/cm. RPS spectra of the sample before and after poling are shown with blue and red lines, respectively. The RPS spectrum of the unpoled sample is also shown in the inset. b) RPS spectra of poled PST as a function of temperature. Green arrows show the thermal evolution of an elastic resonance. c) Temperature dependence of the squared frequency f^2 (red, filled circles) and inverse quality factor Q^{-1} (blue, empty circles) of the elastic resonance. The inverse quality factor, reflecting friction, is given by $Q^{-1} = \Delta f/f$, where Δf is the full width at half maximum. (d) Temperature dependence of RPS peak area (red, filled circles), which represents an effective piezoelectric coefficient, and remnant polarization (blue, open circles) (reproduced from Ref. [52]).

Because paraelectric-ferroelectric transitions correspond to structural changes which generate spontaneous strains, we can always expect an elastic anomaly during the phase transition [22, 62]. Consequently, the depolarization temperature, roughly corresponding to the paraelectric-

ferroelectric transition temperature in $BaTiO_3$ and $PbSc_{0.5}Ta_{0.5}O_3$, is detected by an elastic anomaly related to the depolarization of both compounds. In addition, the contribution of softening from the piezoelectric effect in ceramics can be written as an orientational average of $\mathbf{d}\varepsilon^{-1}\mathbf{d}$, where **d** is the piezoelectric tensor [80]. Since this piezoelectric softening depends on the square of **d**, it does not average out in unpoled ceramics and, if one is able to distinguish other sources of softening around the ferroelectric transitions, such as fluctuations, the elastic softening gives a measure of the piezoelectric response, and hence also of the depolarization, of each domain under its spontaneous polarization, without the need of poling the sample. This has been quantitatively demonstrated at frequencies in the kHz range in $BaTiO_3$ [80], and allows the ferroelectric transition to be probed also in highly conductive $BaTiO_{3-\delta}$ [51, 59], where no dielectric anomaly can be observed [46, 51], but the persistence of the transition is supported by x-ray diffraction [46]. The piezoelectric softening is not evident in the limited temperature range of Fig. 4(a) and 5(c), because the precursor softening from fluctuations may extend for hundreds of kelvins above T_c, and possibly at higher frequency their effect is enhanced. These results can be combined with previous RPS and RUS measurements on ferroelectric $Na_{0.5}Bi_{0.5}TiO_3$ (NBT), where depolarization was also detected by both piezoelectric and elastic anomalies [25]. NBT represents a class of materials whose depolarization is characterized by an intermediate modulated or canted antiferroelectric structure, or a phase mixture between the paraelectric and ferroelectric phases [81, 82, 83]. The depolarization temperature in NBT is also defined as a ferroelectric-relaxor transition [77, 84]. In any case, T_d is associated with a structural change related to the enhancement of in-phase octahedral tilting. Reliability of elastic measurements to determine T_d was previously suggested by Anton *et al*. [7] when T_d is associated with a structural change. Our results indicate that this is the case thanks to simultaneous elastic and piezoelectric

measurements as probed by RPS. Using elastic measurements can be particularly useful in materials where depolarization cannot be probed by conventional dielectric, piezoelectric, and polarization measurements due to conductive nature of materials and may enable the employment of various methods probing mechanical properties [22, 51, 60, 85, 86].

4. Conclusions

RPS is a versatile technique for the measurement of direct and converse piezoelectric effects as a function of temperature with additional capability of *in-situ* electrical poling and providing elastic properties.

The thermal evolution of longitudinal piezoelectric coefficient d_{33} can be accurately determined, which is important for many technological applications where the thermal stability of the piezoelectric coefficient is a priori-condition. It is shown that RPS can be used for quick evaluation of piezoelectric, elastic, and phase transition behavior of poled ferroelectrics. Although not demonstrated here, measurements with direct contact configuration employed here can be carried out between 2 K and 650 K with a suitable furnace.

Finally, the results indicate that elastic measurements are an indirect means to measure the depolarization temperature in ferroelectrics.

Acknowledgements

O.A. thanks the National Natural Science Foundation of China (51850410520) for support. EKHS thanks the EU (861153) and EPSRC (EP/P024904/1) for support. P.S. Silva Jr thanks the Brazilian agencies São Paulo Research Foundation FAPESP (grant #2012/08457-7) and the Coordenação de Aperfeiçoamento de Pessoal de Nível Superior - Brasil (CAPES) - Finance Code 001 (process 88881.062225/2014-01) for support. O.A. thanks Roger W. Whatmore (Imperial College London) for providing the $PbSc_{0.5}Ta_{0.5}O_3$ sample.

APPENDIX

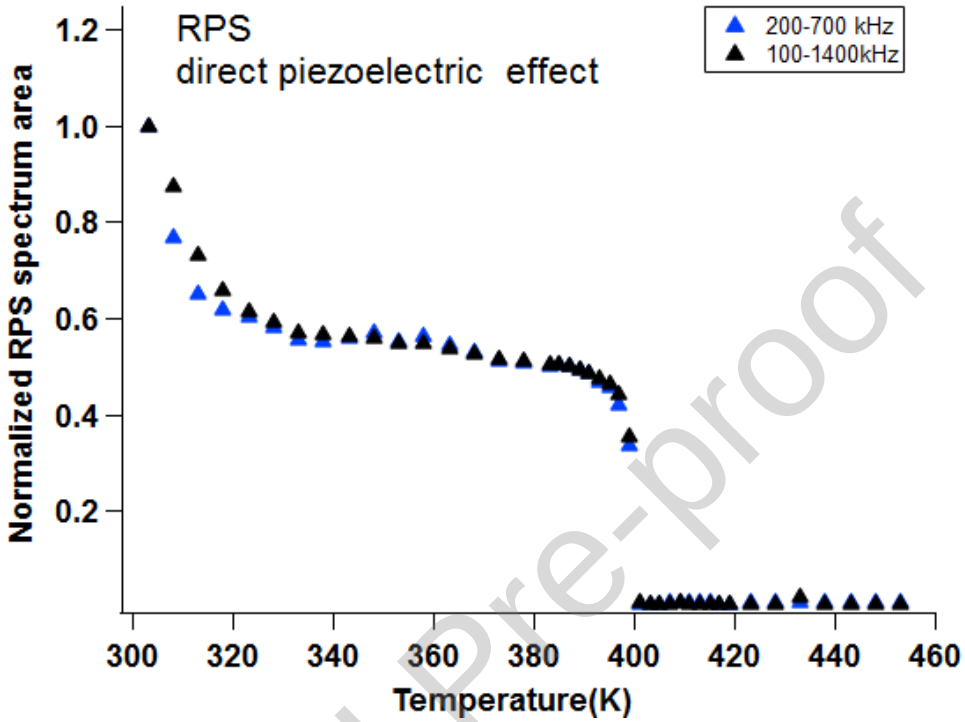

Fig. A1. Comparison of the areas of RPS spectra evaluated between 100-1400 kHz and 200-700 kHz, collected by the direct piezoelectric effect.

References

[1] A. J. Bell, T. P. Comyn, T. J. Stevenson, Expanding the application space for piezoelectric materials, APL Mater. 9 (2021) 010901.

[2] R. W. Whatmore, Y.-M. You, R.-G. Xiong, and C.-B. Eom, 100 years of ferroelectricity—A celebration, APL Mater. 9 (2021) 070401.

[3] T. Zheng, J. G. Wu, D. Q. Xiao, J. G. Zhu, Recent development in lead-free perovskite piezoelectric bulk materials, Prog. Mater. Sci. 98 (2018) 552.

[4] K. Shibata, R. P. Wang, T. Tou, J. Koruza, Applications of lead free piezoelectric materials, MRS Bulletin 43 (2018) 612.

[5] T. Takenaka, H. Nagata, and Y. Hiruma, Current Developments and Prospective of Lead-Free Piezoelectric Ceramics, Jpn. J. Appl. Phys. 47 (2008) 3787.

[6] W. Jo, R. Dittmer, M. Acosta, J. Zang, C. Groh, E. Sapper, K. Wang, J. Rödel, Giant electric-field-induced strains in lead-free ceramics for actuator applications – status and perspective, J. Electroceram 29 (2012) 71.

[7] E.-M. Anton, W.Jo, D. Damjanovic, J. Rödel, Determination of depolarization temperature of $(Bi_{1/2}Na_{1/2})TiO_3$-based lead-free piezoceramics, J. Appl. Phys. 110 (2011) 094108.

[8] J. Walker, H. Ursic, A. Bencan, B. Malic, H. Simons, I. Reaney, G. Viola, V. Nagarajan, T. Rojac, Temperature dependent piezoelectric response and strain–electric-field hysteresis of rare-earth modified bismuth ferrite ceramics, J. Mater. Chem. C. 4 (2016) 7859.

[9] Z. Huang, Q. Zhang, S. Corkovic, R. Dorey, R. W. Whatmore, Comparative measurements of piezoelectric coefficient of PZT films by Berlincourt, interferometer, and vibrometer methods, IEEE Trans. Ultrason., Ferroelectr., Freq. Control 53 (2006) 2287.

[10] J. Fialka, P. Beneš, Comparison of Methods for the Measurement of Piezoelectric Coefficients, IEEE Trans. Instrum. Meas. 62 (2013) 1047.

[11] K. M. Rittenmyer, P. S. Dubbelday, Direct measurement of the temperature- dependent piezoelectric coefficients of composite materials by laser Doppler vibrometry, J. Acoust. Soc. Am. 91 (1992) 2254.

[12] C. C Huang, K. Cai, Y. C. Wang, Y. Bai, D. Guo, Revealing the real high temperature performance and depolarization characteristics of piezoelectric ceramics by combined in situ techniques, J. Mater. Chem. C 6 (2018) 1433.

[13] H. Y. Zhao, Y. D. Hou , M. P. Zheng, X. L. Yu, X. D. Yan, L. Li, M. K Zhu, Revealing the origin of thermal depolarization in piezoceramics by combined multiple in-situ techniques, Mater. Lett. 236 (2019) 633.

[14] D. K. Khatua, A. Mishra, N. Kumar, G. D. Adhikary, U. Shankar, B. Majumdar, R. Ranjan, A coupled microstructural-structural mechanism governing thermal depolarization delay in $Na_{0.5}Bi_{0.5}TiO_3$-based piezoelectrics, Acta Materialia 179 (2019) 49.

[15] E. K. H. Salje, O. Aktas, M. A. Carpenter, V. V. Laguta, J. F. Scott, Domains within domains and walls within walls: Evidence for polar domains in cryogenic $SrTiO_3$, Phys. Rev. Lett. 111 (2013) 247603.

[16] H. Yokota, C. R. S. Haines, S. Matsumoto, N. Hasegawa, M. A. Carpenter, Y. Heo, A. Marin, E. K. H. Salje, Y.Uesu, Domain wall generated polarity in ferroelastics: Results from resonance piezoelectric spectroscopy, piezoelectric force microscopy, and optical second harmonic generation measurements in $LaAlO_3$ with twin and tweed microstructures, Phys. Rev. B 102 (2020) 104117.

[17] G. F. Nataf, M. Guennou, J. Kreisel, P. Hicher, R. Haumont, O. Aktas, E. K. H. Salje, L. Tortech, C. Mathieu, D. Martinotti, N. Barrett, Control of surface potential at polar domain walls in a nonpolar oxide, Phys. Rev. Mater. 1 (2017) 074410.

[18] O. Aktas, M. A. Carpenter, E. K. H. Salje, Polar precursor ordering in $BaTiO_3$ detected by resonant piezoelectric spectroscopy, Appl. Phys. Lett. 103 (2013) 142902.

[19] O. Aktas, S. Crossley, M. A. Carpenter, E. K. H. Salje, Polar correlations and defect-induced ferroelectricity in cryogenic $KTaO_3$, Phys. Rev. B 90 (2014) 165309.

[20] O. Aktas, M. Kangama, G. Linyu, X. Ding, M. A. Carpenter, E. K. H. Salje, Probing the dynamic response of ferroelectric and ferroelastic materials by simultaneous detection of elastic and piezoelectric properties, J. Alloys and Compounds 903 (2022) 163857.

[21] A. Migliori, J. L. Sarrao, Resonant ultrasound spectroscopy: applications to physics, materials measurements, and nondestructive evaluation, Wiley, 1997.

[22] M. A. Carpenter, Static and dynamic strain coupling behaviour of ferroic and multiferroic perovskites from resonant ultrasound spectroscopy, J. Phys.: Condens. Matter 27 (2015) 263201.

[23] O. Aktas, M. Kangama, G. Linyu, G. Catalan , X. Ding, A. Zunger, E. K. H. Salje, Piezoelectricity in nominally centrosymmetric phases, Phys. Rev. Res. 3 (2021) 043221.

[24] O. Aktas, E. K. H. Salje, S. Crossley, G. I. Lampronti, R. W. Whatmore, N. D. Mathur, M. A. Carpenter, Ferroelectric precursor behavior in $PbSc_{0.5}Ta_{0.5}O_3$ detected by field-induced resonant piezoelectric spectroscopy, Phys. Rev. B 88 (2013) 174112.

[25] O. Aktas, J.R. Duclère, S. Quignon, G. Troliard, E. K. H. Salje, Polarity of modulated $Na_{0.5}Bi_{0.5}TiO_3$ and its slow structural relaxation, Appl. Phys. Lett. 113 (2018) 032901.

[26] R. E. A. McKnight, T. Moxon, A. Buckley, P. A. Taylor, T. W. Darling, M. A. Carpenter, Grain size dependence of elastic anomalies accompanying the α–β phase transition in polycrystalline quartz, J. Phys.: Condens. Matter 20 (2008) 075229.

[27] J. Schreuer, B. Hildmann, H. Schneider, Elastic Properties of Mullite Single Crystals up to 1400°C, J. Am. Ceram. Soc. 89 (2006) 1624.

[28] Yougui Liao, Practical electron microscopy and database (2006).

[29] N. A. Hill, Why are there so few magnetic ferroelectrics?, J. Phys. Chem. B 104 (2000) 6694.

[30] B. Jaffe, R.W. Cook Jr, H. Jaffe, Piezoelectric Ceramics, Academic Press Inc (1971).

[31] P. F. Li, W. Q. Liao, Y. Y. Tang, W. C. Qiao, D. W. Zhao, Y. Ai, Y. F. Yao, R. G.Xiong, Organic enantiomeric high- Tc ferroelectrics, PNAS 116 (2019) 5878.

[32] S. T.-McKinstry, S. Zhang, A. Bell, X. Tan, High-performance piezoelectric crystals, ceramics, and films, Annu. Rev. Mater. Res. 48 (2017) 191.

[33] S. Horiuchi, Y. Tokura, Organic Ferroelectrics, Nat. Mater. 7 (2008) 357.

[34] S. V. Trukhanov, A. V. Trukhanov, V. A. Turchenko, A. V. Trukhanova, E. L. Trukhanova, D. I. Tishkevich, V. M. Ivanov, T. I. Zubarg, M. Salema, V. G. Kostishyna, L. V. Paninaa, D. A.

Vinnikb, S. A. Gudkova, Polarization origin and iron positions in indium doped barium hexaferrites, Cer. Inter. 44 (2018) 290.

[35] A. Von Hippel, R.G. Breckenridge, F.G. Chesley, L. Tisza, High dielectric constant ceramics, Ind. Eng. Chem. 38 (1946) 1097.

[36] W. J. Merz, The electric and optical behavior of $BaTiO_3$ single-domain crystals, Phys. Rev. 76 (1949) 1221.

[37] C. Zhao, Y. Huang, J. Wu, Multifunctional barium titanate ceramics via chemical modification tuning phase structure, InfoMat. 2 (2020) 1163.

[38] B. Wang, Y. Gu, S. Zhang, L. Q. Chen, Flexoelectricity in solids: Progress, challenges, and perspectives, Prog. Mater. Sci. 106 (2019) 100570.

[39] S. V. Trukhanov, A. V. Trukhanov, M. M. Salem, E. L. Trukhanova, L. V. Panina, V. G. Kostishyn, M. A. Darwish, A. V. Trukhanov, T. I. Zubar, D. I. Tishkevich, V. Sivakov, D. A. Vinnik, S. A. Gudkova, C. Singh, Preparation and investigation of structure, magnetic and dielectric properties of $(BaFe_{11.9}Al_{0.1}O_{19})_{1-x}$ - $(BaTiO_3)_x$ bicomponent ceramics, Ceram. Int. 44 (2018) 21295.

[40] D. V. Karpinsky, M. V. Silibin, S. V. Trukhanov, A. V. Trukhanov, A. L. Zhaludkevich, S. I. Latushka, D. V. Zhaludkevich, V. A. Khomchenko, D. O. Alikin, A. S. Abramov, T. Maniecki, W. Maniukiewicz, M. Wolff, V. Heitmann, A. L. Kholkin, Peculiarities of the crystal structure evolution of $BiFeO_3$-$BaTiO_3$ ceramics across structural phase transitions, Nanomaterials-Basel 10 (2020) 80112.

[41] C. G. F. Stenger, F. L. Scholten, A. J. Burggraaf, Ordering and diffuse phase transitions in $Pb(Sc_{0.5}Ta_{0.5})O_3$ ceramics, Solid State Commun. 32 (1979) 989.

[42] N. Setter, L. E. Cross, The role of B- site cation disorder in diffuse phase transition behavior of perovskite ferroelectrics J. Appl. Phys. 51 (1980) 4356.

[43] N. M. Shorrocks, R. W. Whatmore, P. C. Osbond, Lead scandium tantalate for thermal detector applications, Ferroelectrics 106 (1990) 387.

[44] S. Crossley, B. Nair, R. W. Whatmore, X. Moya, N. D. Mathur, Electrocaloric Cooling Cycles in Lead Scandium Tantalate with True Regeneration via Field Variation, Phys. Rev. X 9 (2019) 041002.

[45] Y. Nouchokgwe, P. Lheritier, C.-H. Hong, A. Torelló, R. Faye, W. Jo, C. R. H. Bahl, & E. Defay, Giant electrocaloric materials energy efficiency in highly ordered lead scandium tantalate, Nat. Commun. 12 (2021) 3298.

[46] A. Sagdeo, A. Nagwanshi, P. Pokhriya, A.K. Sinha, O. Rajput, V. Mishra, P.R. Sagdeo P, Disappearance of dielectric anomaly in spite of presence of structural phase transition in reduced $BaTiO_3$: Effect of defect states within the bandgap, J. Appl. Phys.123 (2018) 161424.

[47] F. Chu, I. M. Reaney, N. Setter, Role of Defects in the Ferroelectric Relaxor lead Scandium Tantalate, J. Am. Cer. Soc. 78 (1995) 1947.

[48] Y. Tan, J. Zhang , Y. Wu , C. Wang , V. Koval , B. Shi , H. Ye, R. McKinnon, G. Viola, H. Yan, Unfolding grain size effects in barium titanate ferroelectric ceramics, Sci. Rep. 5 (2015) 9953.

[49] F. Yang, Y. Hu, Q. Hu, S. Steiner, T. Frömling, L. Li, P. Wu, E. Pradal-Velázquez, D. C. Sinclair, Dramatic impact of the TiO_2 polymorph on the electrical properties of 'stoichiometric' $Na_{0.5}Bi_{0.5}TiO_3$ ceramics prepared by solid-state reaction, J. Mater. Chem A 10 (2022) 891.

[50] M.A. Almessiere, Y. Slimani, A.V. Trukhanov, A. Baykal, H. Gungunes, E.L. Trukhanova, S.V. Trukhanov, V.G. Kostishin, Strong correlation between Dy^{3+} concentration, structure, magnetic and microwave properties of the $[Ni_{0.5}Co_{0.5}](Dy_xFe_{2-x})O_4$ nanosized ferrites, J. Ind. Eng. Chem. 90 (2020) 251.

[51] F. Cordero, F. Trequattrini, F. Craciun, H. T. Langhammer, D. A. B. Quiroga, P. S. Silva Jr., Probing ferroelectricity in highly conducting materials through their elastic response: Persistence of ferroelectricity in metallic $BaTiO_{3-\delta}$, Phys. Rev. B 99 (2019) 064106.

[52] G. Linyu, F.J. Romero, V. Franco, J.-M. Martín-Olalla, M. Gallardo, E. K. H. Salje, Y. M. Zhou, O. Aktas, Correlations between elastic, calorimetric, and polar properties of ferroelectric $PbSc_{0.5}Ta_{0.5}O_3$ (PST), Appl. Phys. Lett. 115 (2019) 161904.

[53] E. Dul'kin, E.K.H. Salje, O. Aktas, R. W. Whatmore, Ferroelectric precursor behavior in $PbSc_{0.5}Ta_{0.5}O_3$ detected by acoustic emission: tweed and polar nanoregions, Appl. Phys. Lett. 105 (2014) 212901.

[54] K. Kinoshita, A. Yamaji, Grain-size effects on dielectric properties in barium titanate ceramics. J. Appl. Phys. 47 (1976) 371.

[55] T. Hoshina, K. Takizawa, J.Y. Li, T. Kasamai, H. Kakemoto, T.Tsurumi, Domain size effect on dielectric properties of barium titanate ceramics, Jpn. J. Appl. Phys. 47 (2008) 7607.

[56] D. Ghosh , A. Sakata, J. Carter, P. A. Thomas , H. Han, J. C. Nino , J. L. Jones, Domain wall displacement is the origin of superior permittivity and piezoelectricity in $BaTiO_3$ at intermediate grain sizes,Adv. Func. Mater. 24 (2014) 885.

[57] C. A. Randall, N. Kim, J. Kucera, W. W. Cao, T. R. Shrout, Intrinsic and extrinsic size effects in fine-grained morphotropic-phase-boundary lead zirconate titanate ceramics, J. Am. Ceram. Soc. 81 (1988) 677.

[58] T. Hoshina, T. Furuta, T. Yamazaki, H. Takeda, T. Tsurumi, Grain Size Effect on Dielectric Properties of $Ba(Zr,Ti)O_3$ Ceramics, Jap. J. Appl. Phys. 51 (2012) 091004.

[59] F. Cordero, F. Trequattrini, D. A. B. Quiroga, P.S. Silva Jr., Hopping and clustering of oxygen vacancies in $BaTiO_{3-\delta}$ and the influence of the off-centred Ti atoms, J. Alloys and Compounds 874 (2021) 159753.

[60] S. H. Oh, J.-H. Ko, H.-Y. Lee, I. Lazar, K. Roleder, Precursor phenomena of barium titanate single crystals grown using a solid-state single crystal growth method studied with inelastic Brillouin light scattering and birefringence measurements, Molecules 23 (2018) 3171.

[61] J. W. Lee, J.-H. Ko, K. Roleder, D. Rytz, Complete determination of elastic stiffness coefficients and local symmetry breaking in the paraelectric barium titanate, Appl. Phys. Lett. 114 (2019) 072901.

[62] M. A. Carpenter, E. K. H. Salje, Elastic anomalies in minerals due to structural phase transitions, Eur. J. Mineral. 10 (1998) 693.

[63] A. Bencan, E. Oveisi, S. Hashemizadeh, V. K. Veerapandiyan, T. Hoshina, T. Rojac, M. Deluca, G. Drazic, D. Damjanovic. Atomic scale symmetry and polar nanoclusters in the paraelectric phase of ferroelectric materials, Nat. Commun. 12 (2021) 3509.

[64] K. Tsuda, M.Tanaka, Direct observation of the symmetry breaking of the nanometer-scale local structure in the paraelectric cubic phase of $BaTiO_3$ using convergent-beam electron diffraction. Appl. Phys. Exp. 9 (2016) 071501.

[65] K. Wieczorek, A. Ziebiniska, Z. Ujma, K. Szot, M. Górny, I. Franke, J. Koperski, A. Soszyński, K. Roleder, Electrostrictive and piezoelectric effect in $BaTiO_3$ and $PbZrO_3$, Ferroelectrics 336 (2006) 61.

[66] G. R. Fox, J. K. Yamamoto, D. V. Miller, L. E. Cross, S. K. Kurtz, Thermal hysteresis of optical second harmonic in paraelectric $BaTiO_3$, Mater. Lett. 9 (1990) 284.

[67] A. M. Pugachev, V. I. Kovalevskii, N. V. Surovtsev, S. Kojima, S. A. Prosandeev, I. P. Raevski, S. I. Raevskaya, Broken Local Symmetry in Paraelectric $BaTiO_3$ Proved by Second Harmonic Generation, Phys. Rev. Lett. 108 (2012) 247601.

[68] S. Hashemizadeh, A. Biancoli, D. Damjanovic, Symmetry breaking in hexagonal and cubic polymorphs of $BaTiO_3$, J. Appl. Phys. 119 (2016) 094105.

[69] S. Sherrit, B. K. Mukherjee, Characterization of Piezoelectric Materials for Transducers, arXiv:0711.2657 (2007).

[70] An American National Standard: IEEE Standard on Piezoelectricity, The Institute of Electrical and Electronics Engineers, ANSI/IEEE Std 176-1987, New York.

[71] A. M. González, Á. García, C. Benavente-Peces, L. Pardo, Revisiting the Characterization of the Losses in Piezoelectric Materials from Impedance Spectroscopy at Resonance, Materials 9 (2016) 72.

[72] F. Chen, L. Kong, W. Song, C. Jiang, S. Tian, F. Yu, L. Qin, C. Wang, X. Zhao, The electromechanical features of $LiNbO_3$ crystal for potential high temperature piezoelectric applications, J. Materiometrics 5 (2019) 73.

[73] D. Damjanovic, Hysteresis in piezoelectric and ferroelectric materials, The Science of Hysteresis 3 (2005) 337.

[74] D. Damjanovic, M. Demartin, Contribution of the irreversible displacement of domain walls to the piezoelectric effect in barium titanate and lead zirconate titanate ceramics, J. Phys.: Condens. Matter 9 (1997) 4943.

[75] S. V. Kalinin, B. Mirman, E. Karapetian, Relationship between direct and converse piezoelectric effect in a nanoscale electromechanical contact, Phys. Rev. B 76 (2007) 212102.

[76] D. Damjanovic (Swiss Federal Institute of Technology Lausanne), 2022 (private communication).

[77] M. Davies, E. Aksel, J. L. Jones, Enhanced High-Temperature Piezoelectric Coefficients and ThermalStability of Fe- and Mn-Substituted $Na_{0.5}Bi_{0.5}TiO_3$ Ceramics, J. Am. Ceram. Soc. 94 (2011) 1314.

[78] L. M. Garten, S. T.-McKinstry, Enhanced flexoelectricity through residual ferroelectricity in barium strontium titanate, J. Appl. Phys. 117 (2015) 094102.

[79] D. Pesquera, B. Casals, J. E. Thompson, G. F. Nataf, X. Moya, and M. A. Carpenter, Elastic anomalies associated with domain switching in $BaTiO_3$ single crystals under in situ electrical cycling, APL Mater. 7 (2019) 051109.

[80] F. Cordero, Quantitative evaluation of the piezoelectric response of unpoled ferroelectric ceramics from elastic and dielectric measurements: Tetragonal $BaTiO_3$, J. Appl. Phys. 123 (2018) 094103.

[81] X. L. Tan, C. Ma, J. Frederick, S. Beckman, K. G. Webber, The Antiferroelectric↔ Ferroelectric Phase Transition in Lead-Containing and Lead-Free Perovskite Ceramics, J. Am. Ceram. Soc. 94 (2011) 4091.

[82] V. Dorcet, G. Trolliard, P. Boullay, Revisiting the Characterization of the Losses in Piezoelectric Materials from Impedance Spectroscopy at Resonance, Chem. Mater. 20 (2008) 5061.

[83] J. Suchanicz, M. N.-Malczyk, A. Kania, A. Budziak, K. Kluczewska-Chmielarz, P. Czaja, D. Sitko, M. Sokolowski, A. Niewiadomski, T. V. Kruzina, Effects of electric field poling on structural, thermal, vibrational, dielectric and ferroelectric properties of $Na_{0.5}Bi_{0.5}TiO_3$ single crystals, J. Alloys and Compounds 854 (2021) 157227.

[84] A. R. Paterson, H. Nagata , X. Tan , J. E. Daniels, M. Hinterstein , R. Ranjan , P. B. Groszewicz , W. Jo , J. L. Jones, Relaxor-ferroelectric transitions: Sodium bismuth titanate derivatives, MRS Bull. 43 (2018) 600.

[85] G. Polizos, V. Tomer, E. Manias, C. A. Randall, Epoxy-based nanocomposites for electrical energy storage. II: Nanocomposites with nanofillers of reactive montmorillonite covalently-bonded with barium titanate, J. Appl. Phys. 108 (2010) 074117.

[86] G. Quirion, M. L. Plumer, O. A. Petrenko, G. Balakrishnan, C. Proust, Magnetic phase diagram of magnetoelectric $CuFeO_2$ in high magnetic fields, Phys. Rev. B 80 (2009) 064420.

CRediT authorship contribution statement

H. Zhengwang: Investigation; Writing-reviewing, editing; **O. Aktas**: Conceptualization, Writing-original draft; **G. Linyu**: Investigation; **L.-N. Liu:** Investigation; **P. S. da Silva Jr.:** Writing-reviewing, editing; **F. Cordero:** Writing-reviewing, editing; **X.-M. Chen:** Writing-reviewing, editing; **X. Ding**: Writing-reviewing; **E. K.H. Salje:** Writing-reviewing, editing

Declaration of interests

☒ The authors declare that they have no known competing financial interests or personal relationships that could have appeared to influence the work reported in this paper.

Highlights

- RPS is a versatile and complementary technique for measuring depolarization in ferroelectrics.
- The thermal evolution of longitudinal piezoelectric coefficient d_{33} can be accurately determined, which is important for many technological applications where the thermal stability of the piezoelectric coefficient is a priori-condition.
- Thanks to the simultaneous measurement of piezoelectric and elastic properties in RPS, it has been shown that elastic measurements are an indirect means to measure the depolarization temperature in ferroelectrics.